THE JOURNAL OF BIOLOGICAL CHEMISTRY VOL. 284, NO. 50, pp. 34849–34860, December 11, 2009

GRASP65 and GRASP55 Sequentially Promote the Transport of C-terminal Valine-bearing Cargos to and through the Golgi Complex*[S]

Received for publication, September 21, 2009, and in revised form, October 15, 2009 Published, JBC Papers in Press, October 19, 2009, DOI 10.1074/jbc.M109.068403

Giovanni D'Angelo[‡§], Libera Prencipe[‡], Luisa Iodice[‡¶], Galina Beznoussenko[§], Marco Savarese[‡], PierFrancesco Marra[§‖], Giuseppe Di Tullio[§], Gianluca Martire[‡¶], Maria Antonietta De Matteis[§], and Stefano Bonatti[‡1]

From the [‡]Department of Biochemistry and Medical Biotechnology, University of Naples Federico II, 80131 Naples, Italy, the [§]Consorzio Mario Negri Sud, 66030 Santa Maria Imbaro, Italy, the [¶]Department of Environmental Sciences and Technology, University of Molise, 86090 Isernia, Italy, and the [‖]Section of Cell and Molecular Biology, Chester Beatty Laboratories, Institute of Cancer Research, London SW3 6JB, United Kingdom

The Golgi matrix proteins GRASP65 and GRASP55 have recognized roles in maintaining the architecture of the Golgi complex, in mitotic progression and in unconventional protein secretion whereas, surprisingly, they have been shown to be dispensable for the transport of commonly used reporter cargo proteins along the secretory pathway. However, it is becoming increasingly clear that many trafficking machineries operate in a cargo-specific manner, thus we have investigated whether GRASPs may control the trafficking of selected classes of cargo. We have taken into consideration the C-terminal valine-bearing receptors CD8α and Frizzled4 that we show bind directly to the PSD95-DlgA-zo-1 (PDZ) domains of GRASP65 and GRASP55. We demonstrate that both GRASPs are needed sequentially for the efficient transport to and through the Golgi complex of these receptors, thus highlighting a novel role for the GRASPs in membrane trafficking. Our results open new perspectives for our understanding of the regulation of surface expression of a class of membrane proteins, and suggests the causal mechanisms of a dominant form of autosomal human familial exudative vitreoretinopathy that arises from the Frizzled4 mutation involving its C-terminal valine.

GRASP65 and GRASP55 were identified in *in vitro* assays as factors that are required for the stacking of the Golgi cisternae (1, 2). This activity arose as the result of the tethering functions displayed by GRASP65 and GRASP55, through their interactions with their partner proteins GM130 and golgin-45, respectively (2–4). Several other studies have shown more recently that the GRASPs are involved in the maintenance of the structure of the Golgi ribbon in mammal cells during interphase, in controlling the fragmentation of the Golgi complex at the onset of mitosis (5–8), in establishing cell polarity in migrating cells (9), and in the consumption of COPII vesicles and the formation of the *cis*-Golgi in yeast (10).

Although the role of the GRASPs in control of the Golgi complex structure (both in interphase and during mitosis) is well established, their involvement in cargo transport along the secretory pathway is still debated. Indeed, a direct role for GRASPs in cargo transport has so far been established only for the unconventional secretion routes in *Dictyostilium* and *Drosophila* (11, 12), whereas they have been shown not to be directly involved in the trafficking of commonly studied reporter cargo proteins along the "conventional" secretory pathway (*e.g.* the temperature-sensitive (ts-045) mutant of the G protein of vesicular stomatitis virus (VSVG)[2]) and secretory horseradish peroxidase (5, 6, 13, 14). GRASPs can engage different types of interactions including the ones mediated by their PDZ domains, through which the GRASPs cannot only homodimerize, thus participating in cisternal stacking (15) but can also bind the C-terminal valine motifs (C-TVM) of membrane proteins such as pro-transforming growth factor α and p24a (16, 17).

Interestingly a C-terminal valine can behave as "transport signal" in some cargos, as it has been shown that the removal of this valine can lead to either the block or strong delay in trafficking of the proteins to the plasma membrane (16, 18–23) or to their mislocalization (17). In this context, we have shown that the C-TVM influences the rate of endoplasmic reticulum (ER) to Golgi transport of the CD8α glycoprotein, whereby deletion or substitution of this C-TVM resulted in an ~4-fold decrease in the transport kinetics and impaired the accumulation of CD8α in the intermediate compartment (IC) (23). However, the C-TVM has the potential to interact with diverse sets of cytosolic proteins at different segments of the secretory pathway (COPII, GOPC, GRASPs, and syntenin (16, 24, 25)); as a consequence, the ultimate mechanism responsible for the impaired transport induced by the removal of the C-TVM and the precise site of action of the molecular machineries deciphering the signal in the different cargos have remained undefined.

* This work was supported by grants from the Ministero Università Ricerca Scientifica e Tecnologica (to S. B.), the Italian Association for Cancer Research and Telethon Italia (to A. D. M.), and the Telethon Electron Microscopy Core Facility and by a fellowship from the Fondazione Italiana Ricerca sul Cancro (to G. D. A.).

This paper is dedicated to Stefano Ferrari and Francesco D'Angelo.

[S] The on-line version of this article (available at http://www.jbc.org) contains supplemental "Methods" and Figs. S1 and S2.

[1] To whom correspondence should be addressed: Via S. Pansini 5, 80131 Napoli, Italy. Fax: 39-081-7463205; E-mail: bonatti@unina.it.

[2] The abbreviations used are: VSVG, vesicular stomatitis virus G glycoprotein; C-TVM, C-terminal valine motif; ER, endoplasmic reticulum; ERES, endoplasmic reticulum exit sites; FEVR, familial exudative vitroretinopathy; Fz4, Frizzled4; IC, intermediate compartment; PDZ, PSD95-DlgA-zo-1; GST, glutathione *S*-transferase; CHO, Chinese hamster ovary; siRNA, small interfering RNA; WT, wild type; PIPES, 1,4-piperazinediethanesulfonic acid; COPI, coatomer protein complex I; COPII, coatomer protein complex II; ERGIC, endoplasmic reticulum Golgi intermediate compartment.

With this background, we have investigated here the possibility that the GRASPs may selectively control the transport of neosynthesized C-valine cargos. To this end we have combined the two independent approaches of removing the C-TVM and interfering with the GRASP machinery. We provide biochemical and functional evidence that GRASP65 and GRASP55 bind directly to newly synthesized CD8α in a C-TVM-dependent fashion and show that the GRASPs control two sequential transport steps of CD8α from the ER into the Golgi complex. We also show that a similar mechanism operates for the Frizzled4 receptor (Fz4), which is a membrane-multispanning protein involved in a number of signaling events at the plasma membrane, and is associated with the human familial exudative vitroretinopathy (FEVR), a hereditary ocular disorder (26–28). Altogether, our results demonstrate a novel role for GRASPs in the transport of selected cargo along the conventional secretory pathway, and provide a molecular pathogenetic explanation for the defect underlying a dominant form of human FEVR, which is induced by mistrafficking of a mutated Fz4.

EXPERIMENTAL PROCEDURES

All of the culture reagents were obtained from Sigma. The solid chemical and liquid reagents were obtained from Merck (Darmstadt, Germany), Farmitalia Carlo Erba (Milan, Italy), Serva Feinbiochemica (Heidelberg, Germany), Delchimica (Naples, Italy), and BDH (Poole, United Kingdom). All of the radiochemicals were obtained from PerkinElmer Life Sciences. Protein A-Sepharose CL-4B and the ECL reagents were from Amersham Biosciences.

Antibodies—The following antibodies were used: the OKT8 mouse anti-CD8 monoclonal antibody, from Ortho (Raritan, NJ), the N1 mouse anti-CD8 monoclonal antibody (29), a rabbit anti-ERGIC-53 antibody (30), a rabbit anti-GM130 antibody, a rabbit anti-Sec31 antibody, and a rabbit anti-giantin antibody (31), a mouse anti-hemagglutinin antibody, and a rabbit anti-hemagglutinin antibody from Santa Cruz. The anti-GRASP65 polyclonal antibody was obtained through immunization against a fusion protein between glutathione *S*-transferase (GST) and rat GRASP65 and affinity purified; the anti-GRASP55 polyclonal antibody was a kind gift of Dr. F. Barr. Peroxidase-conjugated anti-mouse and anti-rabbit IgG were from Sigma. Texas Red-conjugated anti-mouse IgG and fluorescein isothiocyanate-conjugated anti-rabbit IgG were from Jackson Immunoresearch Laboratories (West Grove, PA).

Cell Culture, Transfection, Virus Infection, Radiolabeling, Immunoprecipitation, Immunofluorescence Microscopy, and Endoglycosidase H Treatment—Parental FRT cells were grown and transiently transfected as described in Ref. 23. CHO and ldlG cells were grown at 34 °C as described previously (32). Stably expressing cells were obtained after transfection by selection in the presence of G418 (Invitrogen) and screening by indirect immunofluorescence. Propagation of the VSV ts-045 strain and infection were performed as described previously (33). Radiolabeling, preparation of cell extracts, and immunoprecipitation were all performed as reported previously (33). In the two-step immunoprecipitation experiments on radiolabeled cell extracts after the first round of immunoprecipitation with the antibody (anti-GRASP65 or anti-GRASP55), samples were boiled for 15 min in denaturation buffer (150 mM NaCl, 20 mM Tris-HCl, pH 7.2, 1% SDS), subsequently the buffer was adjusted to 150 mM NaCl, 20 mM Tris-HCl, pH 7.2, 0.1% SDS, 1% Triton, and CD8 was immunoprecipitated using the folding-insensitive N1-anti-CD8 monoclonal antibody (33). The cells were grown on glass coverslips and treated for indirect immunofluorescence as described previously (34) and observed under an Axiophot microscope or an LSM 510 confocal laser scanning microscope (Carl Zeiss, Jena, Germany). Image analysis was performed using Zeiss LSM 510 colocalization software. Immunoprecipitated samples were treated with 1,000 units of endoglycosidase H (New England Biolabs) as described previously (33).

SDS-PAGE, Western Immunoblotting, and Far Western Blotting—Proteins were resolved on linear 12.5% polyacrylamide gels, as described previously (33), and then electrophoretically transferred to nitrocellulose filters. The filters were incubated overnight in blocking buffer (5% nonfat dry milk, 0.1% Tween 20 in phosphate-buffered saline), and then with primary antibodies diluted in blocking buffer, and finally with peroxidase-conjugated secondary antibodies. After washing, the bound antibodies were detected by ECL. To quantify the relative amounts of the immunolabeled bands, different exposures of the blots were analyzed with the NIH Image program. Binding to the filters of 0.5 mM purified His fusion protein was carried out for 8 h at 4 °C, and the bound protein was detected with a polyclonal anti-His antibody and a peroxidase-conjugated secondary antibody, as described above.

Ultrathin Cryosectioning and Immunogold Labeling—Cells were fixed with 2% formaldehyde and 0.2% glutaraldehyde in PHEM buffer (60 mM PIPES, 25 mM HEPES, 2 mM $MgCl_2$, 10 mM EGTA, pH 7.4), washed in the same buffer, and collected by centrifugation. The cell pellets were embedded in 10% gelatin, cooled in ice, and cut into 1-mm^3 blocks, at 4 °C. The blocks were infused with 2.3 M sucrose at 4 °C for at least 2 h, and frozen in liquid nitrogen. Thick sections (50–60 nm) were cut at −120 °C using an Ultracut R/FCS (Leica, Milan, Italy) equipped with an antistatic device (Diatome, Fort Washington, PA) and a diamond knife. Ultrathin sections were picked up from a mixture of 1.8% methylcellulose and 2.3 M sucrose (1:1), as described previously (35). The cryosections were collected on formvar/carbon-coated slot copper grids and then incubated with different combinations of rabbit polyclonal and mouse monoclonal antibodies, followed by protein-A-conjugated gold particles of different sizes (36). Double immunolabeling was performed as described previously (36), with optimal combinations of gold particle sizes.

RNA Interference—The siRNAs used were specific for human GRASP65 (NM_031899) and human GRASP55 (NM_015530) and consisted of a mixture of four siRNA duplexes selected using the Dharmacon SMART selection process and SMART pool algorithm. They were obtained from Dharmacon (Lafayette, CO). For RNA interference the COS7 cells were plated for 30% confluence in 24-well plates and transfected with 50 pmol of GRASP65 siRNAs using Oligofectamine (Invitrogen), according to the manufacturer's protocol. For the control, COS7 cells were treated with identical concentrations of transfectant. Forty-eight h after the initial siRNA treatment, the cells

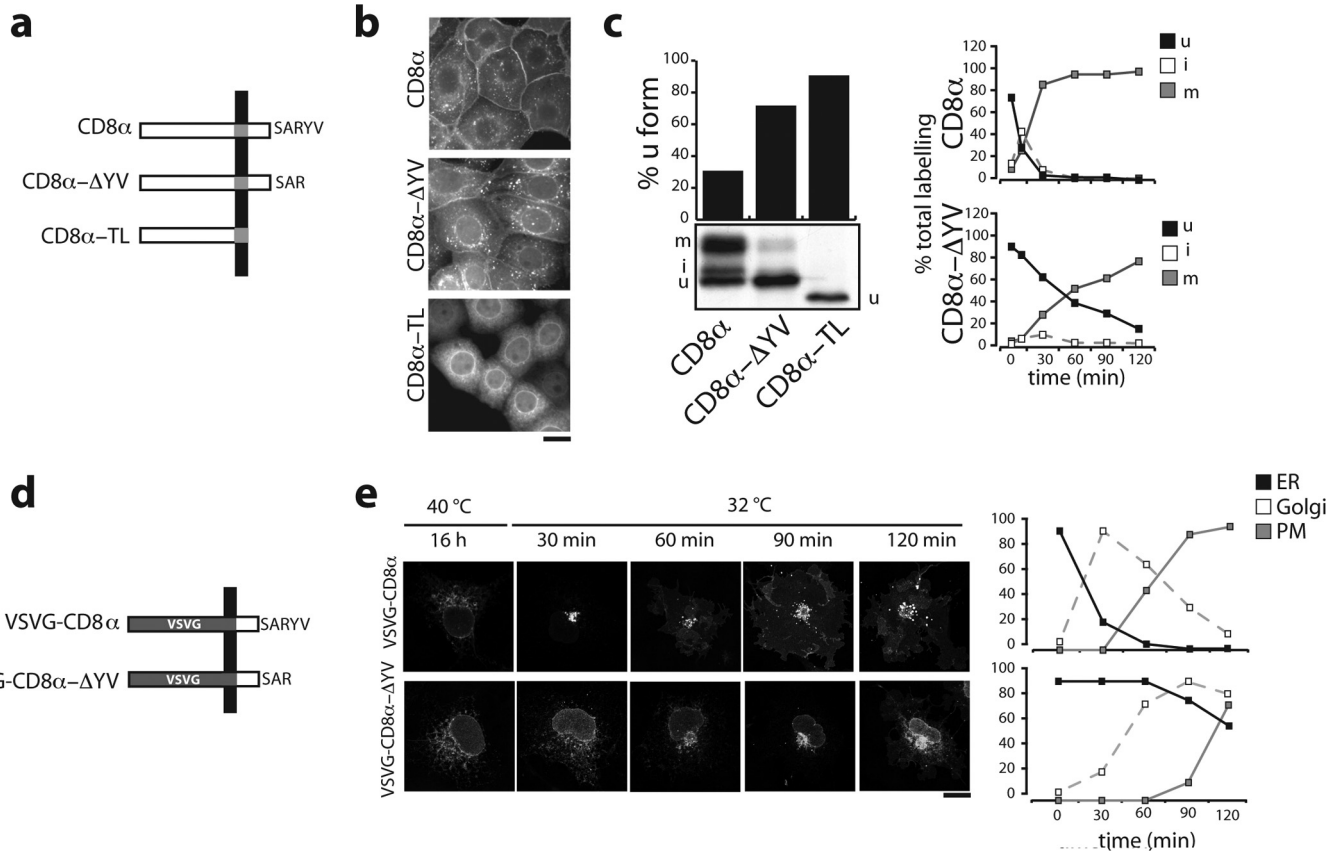

FIGURE 1. **The C-TVM of CD8α enhances its intracellular transport.** *a,* schematic representations of the three different CD8α constructs used. *TL*, tail less. *b*, immunofluorescence analysis of FRT cells stably expressing the CD8α constructs, as indicated. *Bar*, 10 μm. *c*, *left panels*, SDS-PAGE analysis of the immunoprecipitated forms of CD8α and CD8α-ΔYV labeled in stably expressing cells after a 30-min pulse with [^{35}S]Cys/Met. The quantitation of CD8 forms was performed by densitometric scanning and the relative amounts of CD8u (see "Experimental Procedures") are shown in the histogram. The TL mutant shows a faster mobility on SDS-PAGE due to the deletion of the 28-amino acid residues of the cytosolic tail. *Right panels*, time courses of the relative amounts of the immunoprecipitated CD8u, CD8i, and CD8m forms labeled after a 5-min pulse with [^{35}S]Cys/Met followed by the indicated chase times and analyzed by SDS-PAGE. *d*, schematic representations of the VSVG-CD8α and VSVG-CD8α-ΔYV chimeric proteins. *e,* parallel cultures of COS7 cells transfected with these constructs, incubated for 16 h at 40 °C, and then shifted to 32 °C in the presence of cycloheximide for the times indicated, with analysis by confocal immunofluorescence microscopy. The percentages of cells showing ER, Golgi, or plasma-membrane labeling (frequently, more than one compartment was stained in the same cell at a given time point) are shown on the *right* and determined by counting at least 200 cells/condition. The data are from single experiment representative of at least three different experiments, each carried out in duplicate. *Bar*, 10 μm.

were processed directly for immunofluorescence microscopy or transfected with VSVG-based constructs, and kept for 16 h at 40 °C before the transport assays were performed.

RESULTS

The C-TVM Is Required for Rapid Transport of CD8α from the ER to the Golgi Complex—To perform a detailed study of the function of the CD8α C-TVM that we identified previously (23) in cells transiently expressing CD8α, we isolated stable clones of FRT epithelial cells expressing CD8α and two C-terminal-mutated CD8α proteins, CD8α-ΔYV and CD8α-TL. CD8α-ΔYV is a truncated form of CD8α that lacks both the tyrosine at position −2 and the C-terminal valine (our previous work showed that the tyrosine residue plays no role in this C-TVM (23)). The CD8α-TL mutant lacks the entire C-terminal cytosolic tail of CD8α (28 residues) and is severely impaired in its progress along the entire secretory pathway (23); CD8α-TL was chosen as a negative control (Fig. 1*a*).

Immunofluorescence analysis of the clones showed that, at steady state, CD8α is mostly present at the cell surface, whereas CD8α-ΔYV also accumulates in the ER, as indicated by labeling of the nuclear envelope. In contrast, the vast majority of CD8α-TL accumulates in the ER, and is not seen on the cell surface (Fig. 1*b*).

As a glycoprotein, CD8α only has *O*-glycans and moves rapidly from the ER to the plasma membrane ($t_{½}$ 30 min) (37). Its *O*-glycosylation occurs entirely in the Golgi complex and its initial and terminal glycosylation are spatially and temporally separate, occurring in the *cis*- and *trans*-Golgi, respectively. The non-glycosylated (CD8u), initially glycosylated (CD8i), and terminally glycosylated (CD8m) forms of CD8α have different electrophoretic mobilities on SDS-PAGE, thus allowing progression of CD8α along the secretory pathway to be monitored (37).

After a 30-min pulse with [^{35}S]Cys/Met, about 30% of the newly synthesized CD8α WT was in the CD8u form, whereas the majority reached the Golgi complex and were converted to glycosylated CD8i and CD8m forms (Fig. 1*c*, *left panel*). In contrast, the CD8u form represented more than 70 and 80% of CD8α-ΔYV and CD8α-TL, respectively, confirming their slower ER-to-Golgi transport (Fig. 1*c*, *left panel*). In addition, pulse-chase labeling with [^{35}S]Cys/Met showed very fast maturation of non-glycosylated CD8u and an initial transient

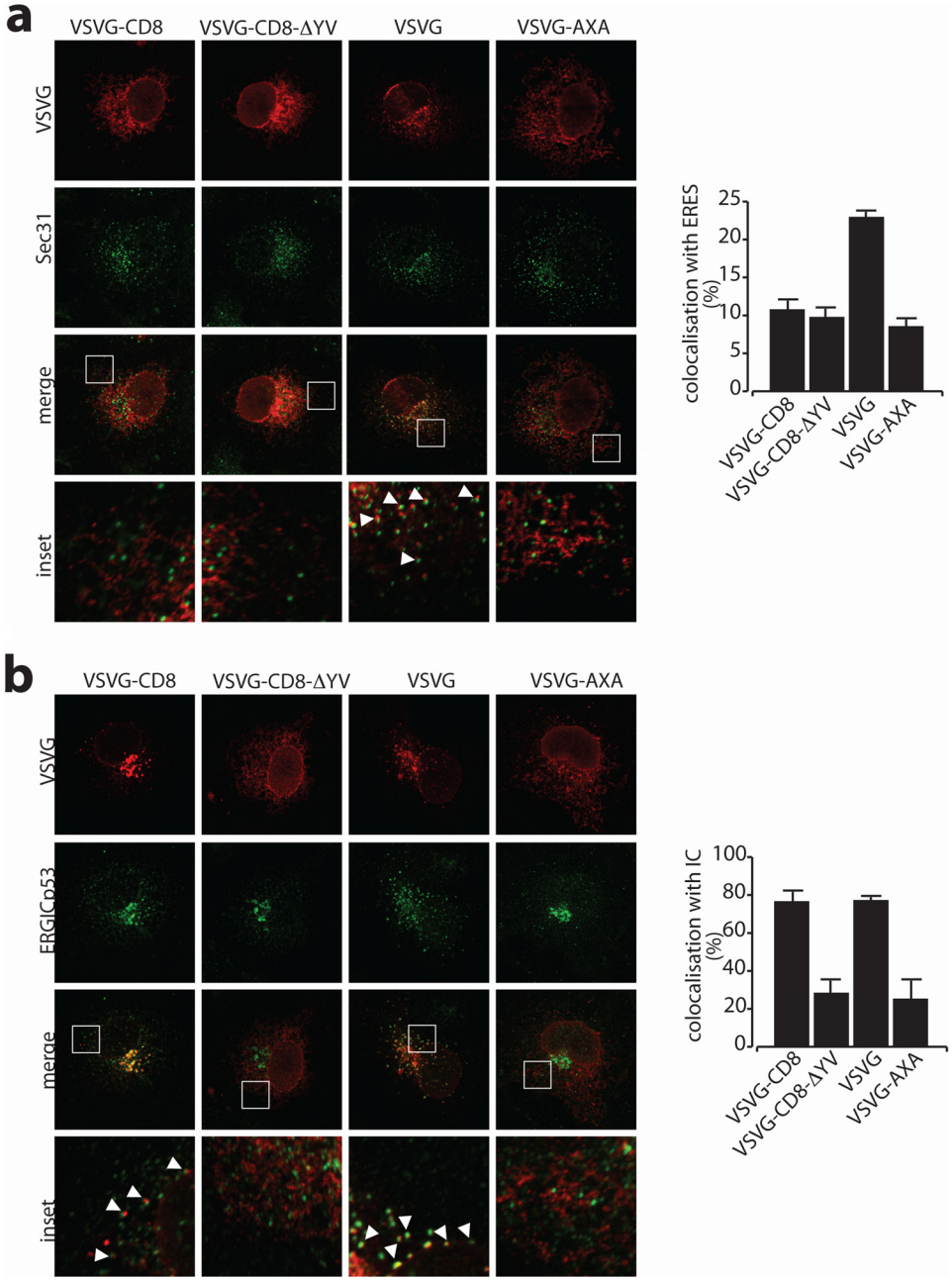

FIGURE 2. **The C-TVM of CD8α promotes the entry or progression into the IC.** *a* and *b*, parallel cultures of COS7 cells transfected with VSVG-CD8α, VSVG-CD8α-ΔYV, VSVG, and VSVG-AXA (no di-acidic tail control) constructs, as indicated (*top*). They were incubated for 16 h at 40 °C, and then shifted to 10 (*a*) and 15 °C (*b*) in the presence of cycloheximide for 3 h, with analysis by confocal immunofluorescence microscopy. Magnifications of the *white boxed areas* in *a* and *b* are shown in the *insets*. The percentages of co-localization with ERES (*a*, Sec31) and IC (*b*, ERGIC-53) are shown on the *right*. For quantitation, images from at least 50 cells were analyzed with LSM-510 software and the values corresponding to the unweighted colocalization of the cargo protein staining into the compartment marker were plotted.

increase of CD8i (Fig. 1*c*, *upper right panel*; CD8u disappearance $t_{½}$ ~12 min) (37); in contrast, CD8α-ΔYV showed delayed glycosylation of CD8u (CD8u disappearance $t_{½}$ ~60 min) and a substantial disappearance of CD8i as a transient intermediate (Fig. 1*c*, *lower right panel*). Thus, the C-TVM promotes a fast and synchronous wave of transport of CD8α to the *cis*-Golgi (23).

To further test this hypothesis, a chimeric reporter protein was generated by joining the ectomembrane and transmembrane domains of the temperature-sensitive VSVG (38) to the cytosolic domain of the CD8α glycoprotein. This reporter should have characteristics of both the viral protein and CD8α: (i) a reversible temperature-sensitive phenotype that causes misfolding and retention of VSVG in the ER at the non-permissive temperature, and its correct folding and exit from the ER upon a shift to the permissive temperature; and (ii) the C-TVM-dependent rapid transport to the Golgi complex of CD8α. Therefore this chimeric reporter protein should allow morphological analysis of its transport.

Two forms of the chimera were generated: one with the wild-type cytosolic tail of CD8α, and the other with this tail but without the terminal tyrosine and valine residues (VSVG-CD8α and VSVG-CD8α-ΔYV, respectively; Fig. 1*d*). Both of these were expressed by transfection in COS7 cells incubated at 40 °C. Confocal immunofluorescence analysis revealed that at this temperature, both chimeric forms of VSVG were retained in the ER (Fig. 1*e*). Upon shifting the temperature to 32 °C, VSVG-CD8α moved quickly to the Golgi complex and then to the plasma membrane, whereas VSVG-CD8α-ΔYV showed accumulation in the ER and a clear delay in its transport to the Golgi complex and plasma membrane (Fig. 1*e*).

The C-TVM of CD8α Stimulates an Early Transport Step between the ER and Golgi Complex—The rate of ER-to-Golgi complex transport of specific cargo proteins has been proposed to be stimulated by selective recruitment to ER exit sites (ERES) via a direct or indirect interaction of the cargo with a COPII coat (24, 39–41). We thus asked whether the C-TVM of CD8α has a role in driving the cargo concentration at the ERES. As a readout for a possible involvement of the C-TVM of CD8α in this process, we considered the subcellular distribution of VSVG-CD8α at 10 °C, a temperature at which COPII components are recruited to the ERES, but where fissioning of the nascent carrier is blocked (42–44). Under these conditions, cargo proteins that can directly interact with COPII components, such as VSVG (which has a COPII-binding DXE di-acidic motif), appear concentrated at the ERES (43) (Fig. 2*a*).

As shown in Fig. 2*a*, VSVG-CD8α showed reduced accumulation at the ERES at 10 °C as compared with the parental VSVG, with a distribution similar to that seen for negative control of the VSVG (VSVG-AXA), in which the di-acidic motif has been mutated (40). VSVG-CD8α-ΔYV also showed reduced accumulation at the ERES at 10 °C, with a distribution very similar to VSVG-CD8α.

As these data indicated that the C-TVM of CD8α does not promote concentration at the ERES, we asked whether this anterograde signal had a role in a subsequent transport step. To this end, we followed the transport of these chimeras at 15 °C, a condition that leads to the accumulation of cargo proteins in the IC (42). Here, with ERGIC-53 used as a marker for the IC, VSVG-CD8α and VSVG showed strong accumulation in the IC (Fig. 2*b*). In contrast, the C-terminal mutant forms VSVG-CD8α-ΔYV and VSVG-AXA showed little IC co-localization, with an overall ER labeling pattern similar to that seen at 10 °C (Fig. 2*b*, compare with Fig. 2*a*). Together, these results suggest that the C-TVM of CD8α promotes a transport step subsequent to cargo recruitment to the ERES and that it fosters cargo entry or proceeds into the IC.

CD8α interacts directly with GRASP65 and GRASP55 through the C-TVM. The requirement of the C-TVM (a PDZ binding motif) for rapid transport of CD8α and concentration at the IC prompted us to test whether GRASP65, which has PDZ domains and cycles between the Golgi complex and pre-Golgi compartments, including the IC, had any role in decoding the CD8α C-TVM, and through this, in controlling trafficking of CD8α.

To this end, we first performed co-immunoprecipitation assays. As shown in Fig. 3*a*, endogenous GRASP65 co-immunoprecipitated with CD8α, but did not co-immunoprecipitate with CD8α-ΔYV, CD8α-TL, or in the control non-transfected parental FRT cells. Fig. 3*a* also shows that GM130, a well known interactor of GRASP65, co-immunoprecipitated with GRASP65 and CD8α; however, p115, an "indirect" interactor of GRASP65 (as it binds the GRASP65/GM130 complex through GM130 (45), was not co-immunoprecipitated with CD8α and was therefore not investigated further (data not shown) (23). Interestingly, as shown in Fig. 3*b*, not only GRASP65, but also GRASP55, which also contains PDZ domains, was co-immunoprecipitated with CD8α, but not with CD8α-ΔYV or CD8α-TL. In addition, the same specific GRASPs-CD8α interactions were revealed when immunoprecipitation was performed with anti-GRASPs antibody (see below). Of note, normal rates of transport of CD8α correlated with its binding to GRASP65, as tested by the concomitant rescue of GRASP binding and rapid transport induced by the readdition of a terminal valine to a CD8α mutant with a partially truncated cytosolic tail (Δ*17*+; Fig. 3*c*) (23).

To determine whether CD8α interacts directly with the GRASPs, far Western blotting assays were performed. The GST-tagged cytosolic tails of CD8α and CD8α-ΔYV, and GST alone, were analyzed by SDS-PAGE. The proteins were transferred to nitrocellulose filters, which were then overlaid with purified His-tagged GRASP65, and GRASP65 lacking its two PDZ domains (ΔPDZ-GRASP65), GRASP55 and FAPP2 (negative control). Finally, binding was revealed with the anti-His epitope antibody.

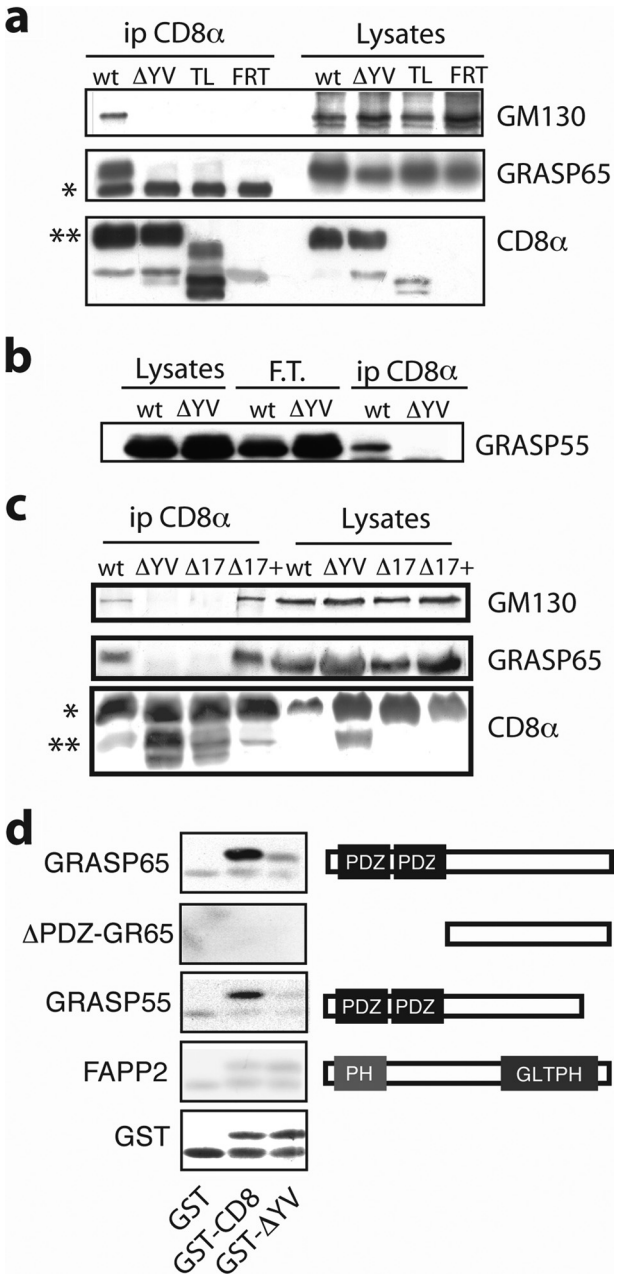

FIGURE 3. **CD8α binds GRASP65 and GRASP55 through the C-TVM.** *a*, cell lysates obtained from parental and stably expressing FRT cells (*FRT*) and FRT cells stably expressing WT CD8α (*wt*), CD8α-TL (*TL*), and CD8α-ΔYV (*ΔYV*) were subjected to immunoprecipitation with an anti-CD8α antibody (*ip CD8α*). The immunoprecipitated products were analyzed by SDS-PAGE, followed by immunoblotting with the antibodies as indicated. Cell lysates (as 1/20) were also loaded (*Lysates*). *, IgG heavy chain; **, CD8m. *b*, cell lysates were treated as in *a*, with the immunoprecipitation performed with an anti-CD8α antibody immobilized on protein A-Sepharose beads. The filter was developed with an anti-GRASP55 antibody. *FT*, unbound material. *c*, cells were transiently transfected to express the different CD8α recombinants, as indicated (*top*). Aliquots of total cell lysates were analyzed directly on SDS-PAGE followed by immunoblotting (*Lysates*, as 1/20), or after immunoprecipitation with an anti-CD8α antibody (*ip CD8α*). The filter was developed with the indicated antibodies. *, CD8m; **, CD8u. *d*, purified GST and GST-tagged cytosolic tails of CD8α and CD8α-ΔYV (GST-CD8α and GST-CD8α-ΔYV, respectively) were resolved on SDS-PAGE, transferred onto a nitrocellulose filter, and incubated with the His-tagged version of the proteins indicated. The bound proteins were revealed with an anti-His antibody. Ponceau staining of the blotted GST-tagged forms is shown *below*. *Right*, schematic representation of the His-tagged proteins used. *PH*, pleckstrin homology domain; *GLTP*, glycolipid transfer protein homology domain. The data are from single experiments representative of at least three independent experiments, each carried out in duplicate.

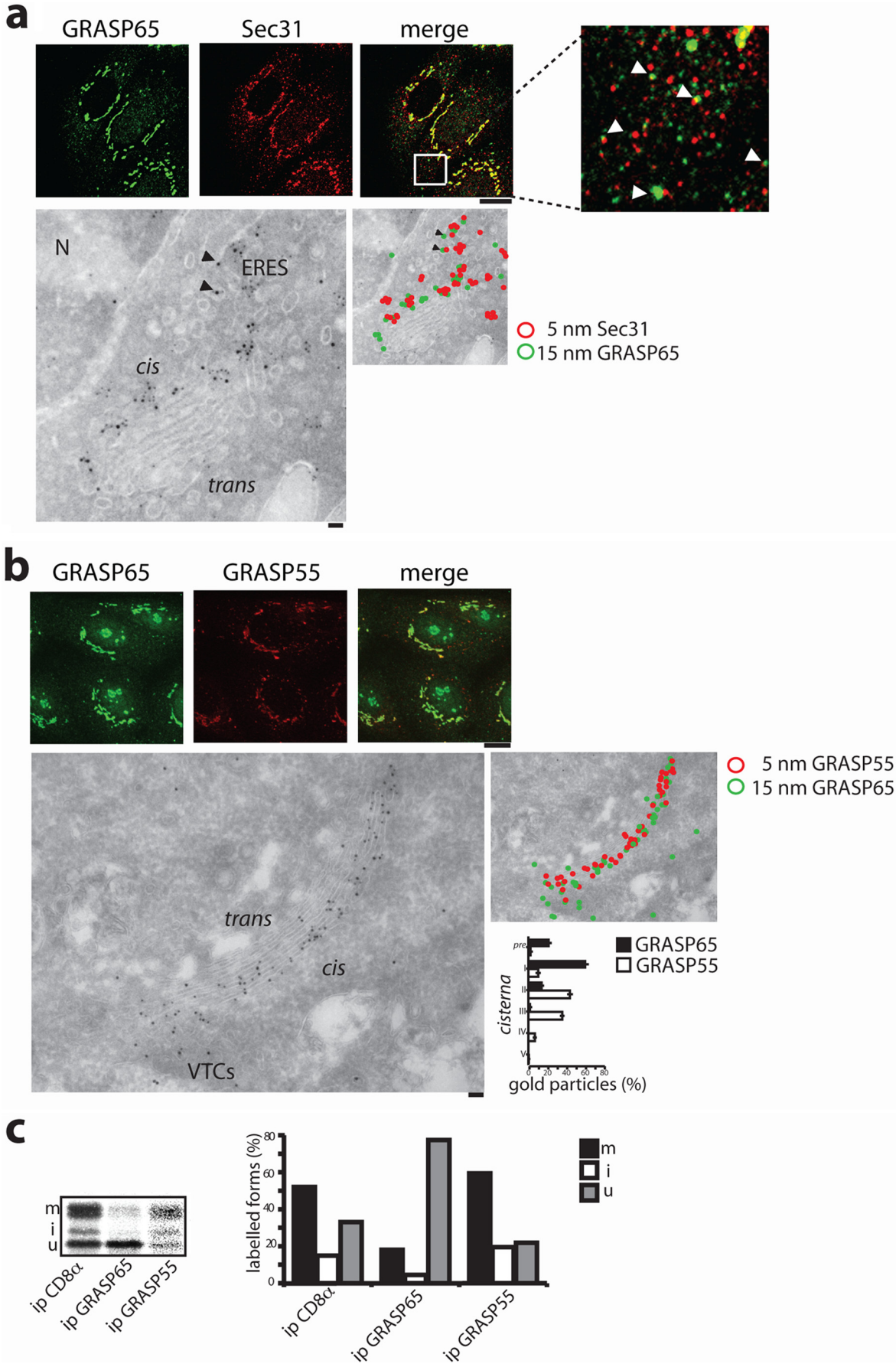
a
GRASP65
Sec31
merge
N
ERES
cis
trans
5 nm Sec31
15 nm GRASP65
b
GRASP65
GRASP55
merge
trans
cis
VTCs
5 nm GRASP55
15 nm GRASP65
GRASP65
GRASP55
cisterna
gold particles (%)
c
m
i
u
ip CD8α
ip GRASP65
ip GRASP55
labelled forms (%)
m
i
u
ip CD8α
ip GRASP65
ip GRASP55

Fig. 3*d* shows that full-length GRASP65 and GRASP55 bind CD8α but not CD8α-ΔYV, whereas neither ΔPDZ-GRASP65 nor FAPP2 showed any significant binding. Thus, the C-TVM of CD8α determines its direct binding to GRASP65 and GRASP55, which is most likely to occur through the PDZ domains of the GRASPs.

GRASP65 and GRASP55 Interact with Different Forms of CD8α—As shown in Fig. 4, and in agreement with a previous report (1), GRASP65 and GRASP55 localize to distinct segments of the secretory pathway. Indeed, at the immunofluorescence level GRASP65 labeling was concentrated in the perinuclear Golgi-like area and peripheral punctae, with distribution similar but not coincident to that of Sec31; GRASP55 appeared instead mostly concentrated in the perinuclear Golgi-like area (Fig. 4*b*). Immunoelectron microscopy showed that GRASP65 was present in the *cis*-Golgi compartments and in elements close to the ER containing Sec31 (*i.e.* ERES) (Fig. 4*a*), whereas GRASP55 was mainly present in the medial cisternae of the Golgi complex (Fig. 4*b*).

Thus, we asked whether neosynthesized CD8α interacts with the two GRASPs at different steps of its intracellular trafficking. To this end cells stably expressing CD8α WT were pulse-labeled for 30 min with [^{35}S]Cys/Met, and then immunoprecipitated with anti-GRASP65 or GRASP55 antibodies. The immunoprecipitates were resuspended and further immunoprecipitated after denaturation with the N1 anti-CD8α monoclonal antibody (see "Experimental Procedures" for details). Importantly, the CD8u (*i.e.* pre-Golgi) form of CD8α was highly enriched in the anti-GRASP65 immunoprecipitate (Fig. 4*c*). In contrast, the CD8m (*i.e.* Golgi) form was enriched in the anti-GRASP55 immunoprecipitate (Fig. 4*c*), indicating that CD8α interacts sequentially with GRASP65 and GRASP55. The interaction with GRASP65 would occur most likely before reaching the Golgi complex, whereas GRASP55 would occur within the Golgi complex, a conclusion fully consistent with the above reported different intracellular localizations of the two GRASPs. This conclusion was also supported by the results of experiments with brefeldin A, a fungal toxin that reversibly disassembles the Golgi complex and arrests the progression of cargos to the Golgi complex. CD8α accumulates in the ER and does not bind GRASP65 in brefeldin A-treated cells, whereas it exits from the ER and quickly recovers its binding to GRASP65 upon brefeldin A washout (data not shown).

GRASP65 and GRASP55 Are Needed for Rapid Transport of CD8α—At this point we used two different approaches to investigate whether the interaction of GRASPs with CD8α had a functional relevance for its transport along the secretory pathway.

First, we evaluated the impact of knocking down the expression of GRASP65 and GRASP55 by RNA interference on CD8α transport. We obtained ~90% knock-down in COS cells for both of the GRASPs (supplemental Fig. S1), with only minor effects on the distribution of the Golgi marker giantin at the immunofluorescence level (data not shown). Mock treated and GRASPs knocked-down cells (KD) were transfected with VSVG-CD8α or VSVG-GFP cDNAs, and incubated at 40 °C for 16 h to arrest the protein in the ER. The temperature was then shifted to 32 °C and transport of the different cargos followed up to 90 min (Fig. 5, *a* and *b*). Although transport of VSVG, in agreement with a previous report (13), was comparable in mock and GRASP-KD cells, the transport of VSVG-CD8α was distinctively delayed in GRASP65- and 55-KD cells compared with mock cells. In particular, at 30 min VSVG-CD8α was still largely present in the ER (and its transport toward the Golgi complex and then to the plasma membrane was delayed) in GRASP65-KD cells; in contrast, in GRASP55-KD cells, transport of VSVG-CD8α appeared undisturbed at 30 min (*i.e.* normal exit from the ER and arrival at the Golgi complex), but was clearly delayed afterward (barely detectable on the plasma membrane at 90 min) (Fig. 5, *a* and *b*). These results indicate that GRASP65 and GRASP55 have specific roles for transport of C-TVM-bearing cargos and confirmed that GRASP55 acts after GRASP65 on these cargos.

To analyze the site of action of the GRASPs in more detail, the transport experiments were repeated shifting the temperature from 40 to 10 °C (concentration at the ERES) or 15 °C (arrival to the IC). No significant differences were seen between mock and GRASP-KD cells at 10 °C (not shown); in contrast, striking differences emerged between GRASP65- and GRASP55-KD cells with the shift to 15 °C: here the transport of VSVG-CD8α to the IC was markedly inhibited in GRASP65-KD cells but not in GRASP55-KD cells. VSVG-GFP was again unaffected (Fig. 5*d*). These results thus fully support the hypothesis that GRASP65 is needed to enter and proceed through the IC, whereas GRASP55 is needed to enter and proceed through the Golgi complex. Further support for these conclusions came from the observation that microinjection of an anti-GRASP65 antibody inhibited the transport of CD8α to the reassemblying Golgi complex in a brefeldin A-washout assay (data not shown).

Next, the requirement for GRASP65 and its main interactor GM130 in CD8α transport was tested in ldlG cells, a conditional-lethal mutant CHO cell line that does not express detectable levels of GM130 (4, 32, 46). Thus, at the non-permissive temperature (39.5 °C), ldlG cells show a complex phenotype that is characterized by the disruption of the Golgi complex and a block in the transport of newly synthesized proteins (32). How-

FIGURE 4. **Intracellular distribution of GRASP65 and GRASP55 and preferential interaction with different CD8α forms.** *a*, immunofluorescence analysis in FRT cells (*upper panels*), and immunoelectron microscopic analysis in RBL cells (*lower panels*) of the distribution of GRASP65 and Sec31 proteins (*bars*, 10 and 100 μm, respectively). *Black arrowheads* indicate GRASP65 labeling at ERES. *b*, as in *a*, but labeling for GRASP55 and GRASP65. The *lower right panel* shows the relative distribution of GRASP65 and GRASP55 over the Golgi complex cisternae as assessed by counting the number of gold particles per cisternae in 30 different Golgi stacks. *c*, FRT cells stably expressing CD8α were pulse-labeled for 30 min with [^{35}S]Cys/Met, and lysed. Five percent of the lysates were immunoprecipitated (*ip*) with an anti-CD8 antibody, as indicated. The remainder was divided in two aliquots and initially immunoprecipitated with anti-GRASP65 or anti-GRASP55 antibody, with the immunoprecipitates resuspended and then immunoprecipitated with the anti-CD8 antibody (indicated as *ip GRASP65* or *GRASP55*). The lane with the anti-GRASP55 immunoprecipitation is from a longer exposure of the gel. The percentage of CD8u, CD8i, and CD8m forms on the total CD8α is indicated on the *right panel*.

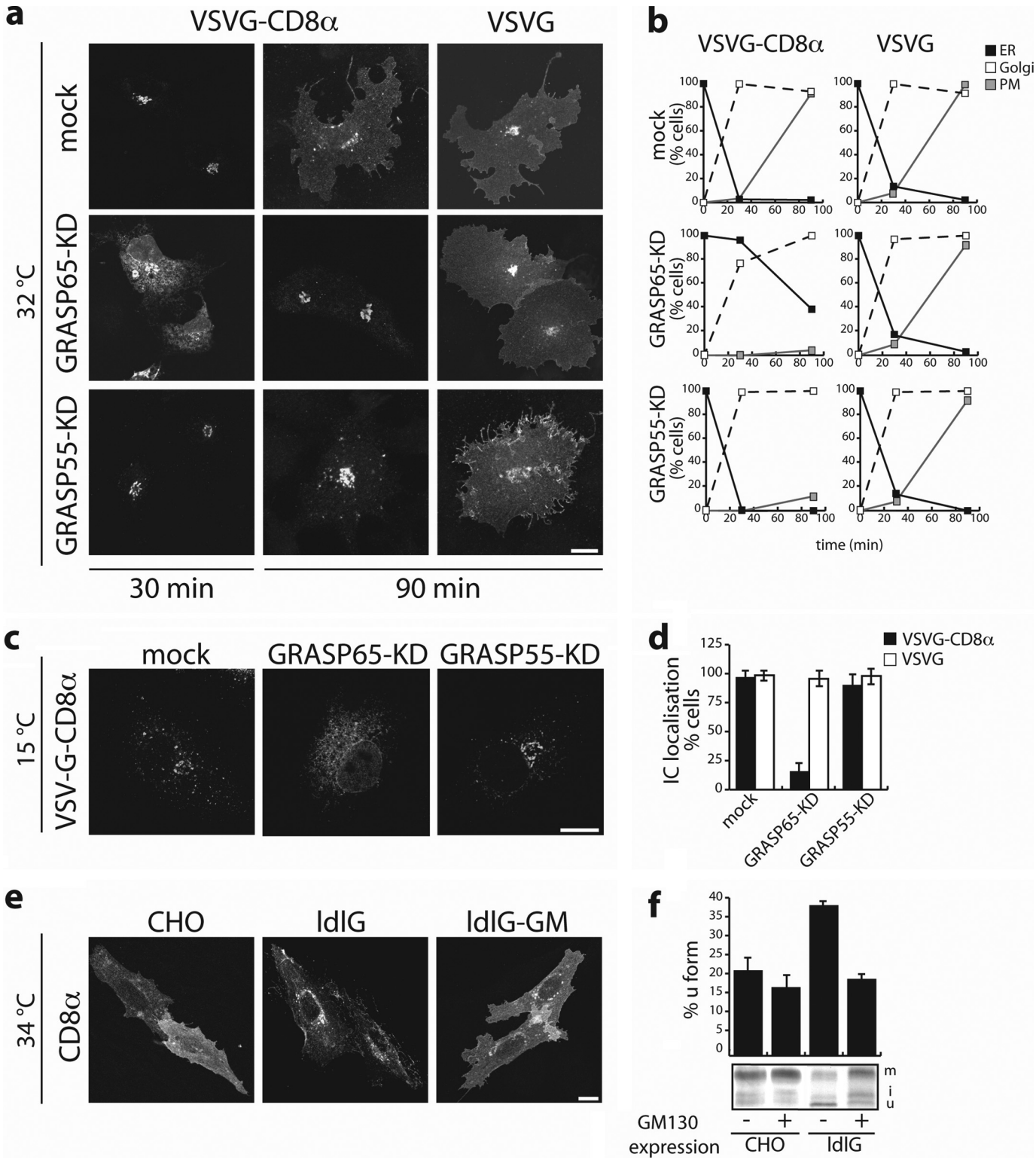

FIGURE 5. **Transport of CD8α is selectively affected when the expression of GRASP65 or GRASP55 is impaired.** *a–d*, parallel cultures of COS7 cells were mock-transfected or transfected with siRNAs pools against GRASP65 and GRASP55, as indicated (*mock*, *KD*) (see also supplemental Fig. S1 and "Experimental Procedures"). Forty-eight hours later, the cells were transfected with VSVG-CD8α and VSVG-GFP cDNAs, as indicated, incubated for 16 h at 40 °C, and then shifted to 32 °C (*a* and *b*) or 15 °C (*c* and *d*) in the presence of cycloheximide for the times indicated (*a* and *b*) or for 3 h (*c* and *d*) with analysis by confocal immunofluorescence microscopy. *a*, representative experiment. *b*, relative ER, Golgi, and plasma-membrane labeling (determined as in Fig. 1*e*). *c*, representative experiment. *d*, accumulation in the IC of the transfected proteins, as indicated. *e*, parallel cultures of parental CHO, ldlG, and ldlG cells stably transfected for expression of GM130 were grown on glass coverslips at 34 °C, transfected to express CD8α, and analyzed by confocal immunofluorescence microscopy. *f*, parallel cultures of parental CHO and ldlG cells were grown at 34 °C and transiently transfected with CD8α alone or CD8α and GM130 cDNAs, and then pulse-labeled with [^{35}S]Cys/Met for 90 min. The cells were then lysed and subjected to immunoprecipitation with an anti-CD8α antibody, and the immunoprecipitates were analyzed by SDS-PAGE. The CD8u, CD8i, and CD8m forms of CD8α are indicated. The relative amounts of the CD8u form were assessed by densitometric scanning, and are given in the histogram. *Bars*, 10 μm. The quantified data are presented as mean ± S.D. from three independent experiments, each carried out in duplicate ($n = 3$).

ever, at 34 °C these cells have an apparently normal phenotype and continue to proliferate, despite the absence of GM130. ldlG cells express GRASP65, although it is delocalized to the periphery even at the permissive temperature (32). Thus we analyzed the intracellular distribution of GRASP65 at 34 °C in parental CHO cells and in these ldlG cells, and in ldlG cells transfected for the expression of exogenous GM130. GRASP65 was indeed completely delocalized, but expression of GM130 led to a clear re-association of GRASP65 with the Golgi complex (not shown) (4). Thus, the parental CHO, the ldlG cells, and the ldlG cells expressing GFP-GM130 were transfected at 34 °C with CD8α cDNA. At steady state, CD8α appeared localized mainly at the cell surface in CHO cells and in ldlG cells stably expressing GFP-GM130, whereas in the ldlG cells (without GM130) it was mainly in the Golgi complex, with less seen at the cell surface (Fig. 5*e*). These CD8α-transfected cells were also analyzed after 90 min of pulse labeling with [^{35}S]Cys/Met, and the percentage distributions of the labeling among the CD8u, CD8i, and CD8m forms of CD8α were analyzed, as described above. The rate of transport of CD8α appeared to be significantly lower in ldlG cells in comparison to the parental CHO cells (increased CD8u; Fig. 5*f*), whereas the expression of GM130 in ldlG cells restored the full rate of transport (Fig. 5*f*). In contrast, and in agreement with previous results (4, 32), no major differences were seen when the transport of the VSVG glycoprotein to the Golgi complex was analyzed in parallel (supplemental Fig. S2).

Transport to the Cell Surface of the Human Fz4 Receptor Requires a C-TVM and Interactions with GRASP65 and GRASP55—To explore whether the results obtained with CD8α have broader implications, we analyzed the transport to the plasma membrane of the Fz4 receptor (Fz4-wt), a member of the Fz receptor family, which is involved in embryogenesis and adult tissue homeostasis (47). Fz4-wt is a seven-transmembrane spanning domain protein with an extracellular amino-terminal domain that is required for ligand binding. It also has short extracellular and intracellular loops that connect the transmembrane segments, and a 41-residue C-terminal cytosolic domain that terminates with two consecutive valines. Recently, a frameshift mutation (L501fsX533) has been described at the fifth cytosolic residue of Fz4-wt, which results in a change in the protein "tail" with a premature stop after 32 residues, and with no final valines (26). This mutant (Fz4-FEVR) is associated with a dominant form of human FEVR, and strikingly, does not reach the plasma membrane in transfected cells (48). Thus, we generated Fz4-FEVR and two other Fz4 constructs, Fz4-ΔVV, as Fz4-wt without only the two terminal valine residues, and Fz4-FEVR-VV, as the Fz4-FEVR disease mutant with two terminal valines re-attached (Fz4-FEVR-VV; Fig. 6*a*). These constructs were transfected in COS7 cells, and their localization determined by confocal immunofluorescence microscopy in comparison to Fz4-wt and Fz4-FEVR.

As shown in Fig. 6, *b* and *c*, Fz4ΔVV showed less accumulation at the cell surface when compared with Fz4-wt, and most strikingly, localization of the Fz4-FEVR mutant at the plasma membrane was rescued almost completely just by the addition of two valine residues at its C terminus (Fz4-FEVR-VV). Moreover, far Western analysis revealed specific valine-dependent binding of the Fz4-wt tail (and also Fz4-FEVR-VV tail) to both GRASP65 and GRASP55 (Fig. 6*d*), and knocking down the expression of either GRASP65 or GRASP55 significantly decreased the amount of Fz4-wt transported to the cell surface (Fig. 6, *e* and *f*). These data were thus all fully consistent with those obtained with CD8α.

DISCUSSION

In the present study, we have shown that GRASP65 and GRASP55 decode the information provided by the C-TVM of CD8α and Fz4 to sequentially promote their anterograde transport along the secretory pathway. Two main lines of evidence support this conclusion, provided by knocking down the GRASPs levels by RNA interference and by using cells defective for the function of GRASP65. On the other hand, mutations of the motif that result in altered transport also lead to the loss of direct binding of CD8α and Fz4 with the GRASPs. Thus, perturbing the GRASPs or removing the C-TVM results in the same transport defect. Strikingly, the GRASPs do not directly contribute to the transport of membrane cargo proteins that do not bear the C-TVM, and thus this mechanism will be specific for a subset of membrane proteins. Therefore, our data provide an explanation for the molecular mechanisms behind the previously reported role of the C-TVMs in anterograde transport (18–21, 23) and for binding of GRASPs to specific cargos (16, 17). Our data also clearly establish that as well as both GRASP65 and GRASP55 having their functions in Golgi architecture, mitotic progression, and unconventional protein secretion, they also have direct roles in the conventional transport of secretory cargo between the ER, IC, and Golgi complex. Finally, our data open up new interesting scenarios for the regulation of surface expression of receptors such as CD8 and Fz4, and they suggest that an alteration in this mechanism is the cause of a dominant form of human FEVR.

What might be the distinctive properties of the C-TVM-bearing cargo proteins that make them sensitive to the GRASPs? Different possibilities can be envisaged here. These proteins might have an as-yet-undefined "retrograde" signal that would usually be overridden by the GRASP-interacting anterograde C-TVM. In the absence of either the valine signal or GRASPs, the retrograde motif would mediate recycling of these cargo proteins to the ER, as has been suggested for the *N*-methyl-D-asparatic acid receptor, where a C-TVM counteracts the activity of an ER retention arginine-based motif in the protein (49, 50). As an additional possible mechanism, the C-TVM could promote an active sorting of these GRASP-sensitive cargo proteins into anterograde moving carriers, thus accelerating their transport to the Golgi complex. In the absence of the C-TVM or GRASPs, these cargos would instead be transported via a bulk-flow mechanism, which would necessarily be less effective than the mechanism based on active sorting.

What are the transport steps that are specifically controlled by this C-TVM/GRASPs interaction? Our model in Fig. 7 illustrates the hypothesis that we believe to be more consistent with the available evidence and results reported here. GRASP65 and GRASP55 are envisaged to have specific functions at two different stages that are temporally and spatially distinct. The

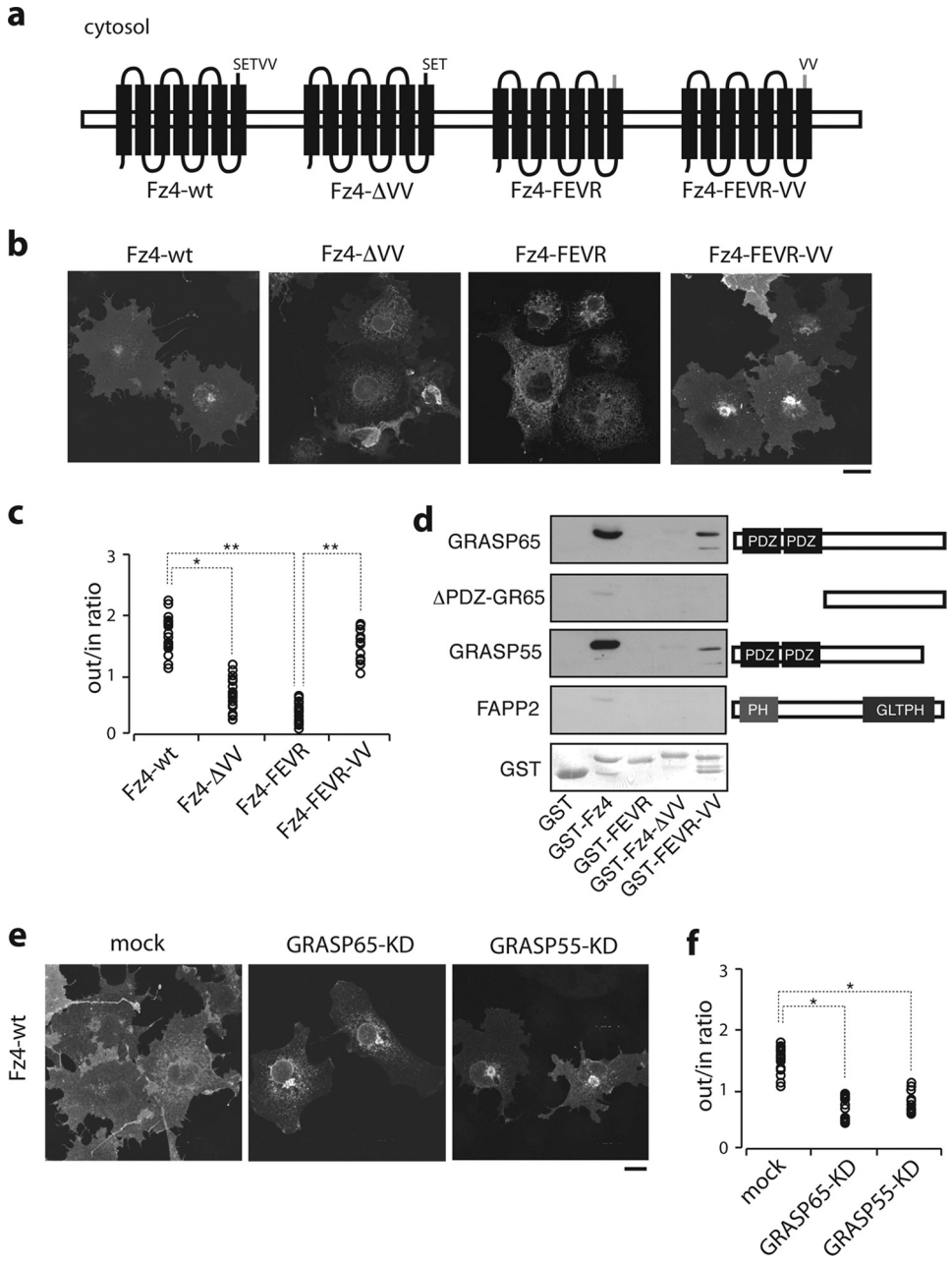

FIGURE 6. **Transport to the cell surface of Fz4 receptor requires C-TVM and GRASPs.** *a*, schematic drawing of the recombinant Fz4 forms used. *b*, parallel cultures of COS7 cells transfected with the Fz4 forms as indicated, with analysis by confocal immunofluorescence microscopy. *c*, cells were transfected as in *b* and stained with a monoclonal anti-hemagglutinin epitope antibody, and then permeabilized. Following permeabilization, cells were stained with a polyclonal anti-hemagglutinin epitope antibody, thus providing quantification of the extracellular *versus* intracellular staining of the transfected cells. *d*, purified GST and GST-tagged cytosolic tails of Fz4, Fz4-FEVR, Fz4-ΔVV, and Fz4-FEVR-VV were resolved on SDS-PAGE, transferred onto a nitrocellulose filter, and incubated with the His-tagged version of the proteins indicated. The bound proteins were revealed with an anti-His antibody. *Right*, schematic representation of the His-tagged forms of GRASP65, GRASP55, the recombinant form of GRASP65 lacking the 2 PDZ domains (ΔPDZ-GR65), and FAPP2 as negative control. Ponceau staining of the blotted GST-tagged forms is shown below. *e*, parallel cultures of COS7 cells were mock-transfected or transfected with siRNAs pools against GRASP65 and GRASP55, as indicated (*mock*, *KD*) (see "Experimental Procedures"). Forty-eight hours later, the cells were transfected to express Fz4-wt, as indicated. *f*, analysis by confocal immunofluorescence microscopy and quantitation as for *b* and *c*. *Bars*, 10 μm; *, $p < 0.05$; **, $p < 0.01$. *PH*, pleckstrin homology domain.

GRASP65-sensitive step corresponds to an early step of ER-to-Golgi transport, different from COPII-mediated recruitment to the ERES (see Fig. 3). Most likely, this step is also different from the budding of carriers from the ER, as it has been reported that in yeast the GRASPs homologue Grh1 is not required for budding of COPII vesicles although it binds COPII (10); and our preliminary results suggest that the C-TVM of CD8α plays no role in a budding assay *in vitro*.[3]

Thus, the site of action of this valine-GRASP65 interaction system has to be placed at a post-ER and pre-Golgi station, *i.e.* the IC, a site where GRASP65 has been shown to recycle from the Golgi complex (31, 51). Unfortunately, at present too little is known at the molecular level about cargo protein entry into and transiting through the IC to define in detail the mechanisms promoting anterograde transport of these C-TVM-bearing proteins. What has so far been established is the compositional heterogeneity of the IC, with its "early" elements that are physically close to but distinct from the ERES, and its "late" elements that are closer to the Golgi complex (31). In this context, active sorting of a cargo protein from the early to the late IC components (through its interaction with GRASP65) would offer a kinetic transport advantage. This would occur through recruitment of the GRASP65-GM130 machinery, which can form a complex with the transiting C-TVM-bearing cargo, and which has a recognized role in promoting the incorporation of ER-derived carriers into the Golgi complex (4) and maintaining the architecture of the Golgi complex itself. However, the relationships between the role of GRASP65 in the transport of C-TVM-bearing cargo proteins that we report here and its established structural role at the Golgi complex remain to be defined.

The GRASP55-sensitive transport step for these GRASP-sensitive cargos appears to be within the Golgi complex, and presumably related to progression within the Golgi complex of the cargos, considering the preferential binding of GRASP55 to the CD8m form (Fig. 4), the block of VSVG-CD8α in a GM130-positive Golgi compartment in GRASP55-KD cells (not shown), and considering

[3] G. D'Angelo, L. Iodice, and S. Bonatti, unpublished data.

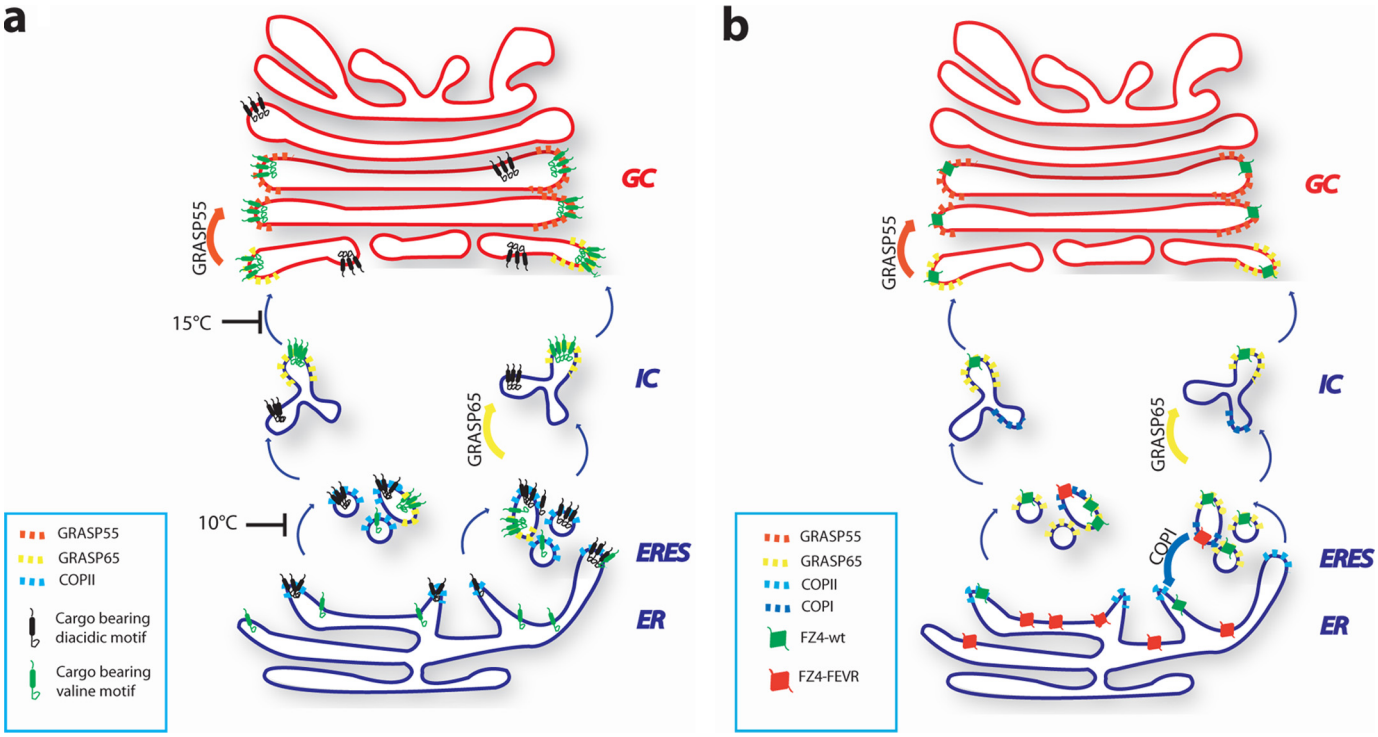

FIGURE 7. **Working model.** *a*, schematic representation of the role of the C-TVM and possible site of action of GRASP65 and GRASP55 proteins in selecting C-TVM-bearing cargo through the early secretory pathway. In the absence of the C-TVM, cargo proceeds in the pathway with a much slower kinetic. In the case of Fz4-FEVR (*b*), we speculate that a retention/recycling motif would either block the protein in the ER or trigger recycling from the IC, possibly driven by COPI vesicular carriers.

the medial Golgi localization of GRASP55 (Fig. 3) (1). The molecular mechanisms involved in this transport block have yet to be defined. An intriguing possibility is that in the absence of GRASP55, the C-TVM-bearing cargo proteins remain bound to GRASP65, and are thus stacked in early Golgi compartments.

Finally, interactions with GRASPs are likely to have an important role in the physiology of CD8 and Fz4, two plasma-membrane receptors. CD8 is a glycoprotein complex mainly expressed in cytotoxic T lymphocytes. It consists of two subunits that can associate as homodimers and heterodimers: the α subunit, which has a C-terminal valine; and the β subunit, which is devoid of this signal (52). CD8$\alpha\beta$ is the main functional co-receptor, although CD8$\alpha\alpha$ is also expressed at the cell surface and is functional, whereas CD8$\beta\beta$ is inactive and retained in the ER (53–57). The co-expression of CD8α relocalizes CD8β to the cell surface (57, 58). Thus this highlights the driving role of the valine signal in the promotion of exposure of these receptors at the plasma membrane, and hence, their function.

Fz4 and the other members of the Fz family of Wnt receptors also form homo-oligomers and hetero-oligomers (48). Recently, it was shown that this oligomerization occurs in the ER (48), and that the Fz4 mutation responsible for a dominant form of FEVR does not allow anterograde transport of the mutated proteins and blocks the transport of the wild-type Fz chains upon oligomerization. This mechanism would explain the dominant effects of the Fz4-FEVR mutant in heterozygous FEVR patients (26). The absence of Fz4 receptor expression at the plasma membrane results in a signaling defect during embryogenesis that leads to defective angiogenesis, aberrant neovascularization, and exudative retinopathy (26–28). Our results now offer a molecular explanation to the intracellular retention of Fz4-FEVR, the inability of the mutant protein to interact with GRASP65 and GRASP55.

Acknowledgments—We thank E. Brescia, M. Santoro, and P. Sesti for technical assistance, C. P. Berrie for editorial assistance, Dr. F. Barr for GRASP55 antibody, Dr. G. De Luca for participating in the initial steps of this work, and Drs. M. R. Hayden and M. L. MacDonald for the Fz4-wt construct.

REFERENCES

1. Shorter, J., Watson, R., Giannakou, M. E., Clarke, M., Warren, G., and Barr, F. A. (1999) *EMBO J.* **18,** 4949–4960
2. Barr, F. A., Puype, M., Vandekerckhove, J., and Warren, G. (1997) *Cell* **91,** 253–262
3. Short, B., Preisinger, C., Körner, R., Kopajtich, R., Byron, O., and Barr, F. A. (2001) *J. Cell Biol.* **155,** 877–883
4. Marra, P., Salvatore, L., Mironov, A., Jr., Di Campli, A., Di Tullio, G., Trucco, A., Beznoussenko, G., Mironov, A., and De Matteis, M. A. (2007) *Mol. Biol. Cell* **18,** 1595–1608
5. Feinstein, T. N., and Linstedt, A. D. (2008) *Mol. Biol. Cell* **19,** 2696–2707
6. Duran, J. M., Kinseth, M., Bossard, C., Rose, D. W., Polishchuk, R., Wu, C. C., Yates, J., Zimmerman, T., and Malhotra, V. (2008) *Mol. Biol. Cell* **19,** 2579–2587
7. Puthenveedu, M. A., Bachert, C., Puri, S., Lanni, F., and Linstedt, A. D. (2006) *Nat. Cell Biol.* **8,** 238–248
8. Sütterlin, C., Hsu, P., Mallabiabarrena, A., and Malhotra, V. (2002) *Cell* **109,** 359–369
9. Bisel, B., Wang, Y., Wei, J. H., Xiang, Y., Tang, D., Miron-Mendoza, M., Yoshimura, S., Nakamura, N., and Seemann, J. (2008) *J. Cell Biol.* **182,** 837–843

10. Behnia, R., Barr, F. A., Flanagan, J. J., Barlowe, C., and Munro, S. (2007) *J. Cell Biol.* **176,** 255–261
11. Schotman, H., Karhinen, L., and Rabouille, C. (2008) *Dev. Cell* **14,** 171–182
12. Kinseth, M. A., Anjard, C., Fuller, D., Guizzunti, G., Loomis, W. F., and Malhotra, V. (2007) *Cell* **130,** 524–534
13. Sütterlin, C., Polishchuk, R., Pecot, M., and Malhotra, V. (2005) *Mol. Biol. Cell* **16,** 3211–3222
14. Kondylis, V., Spoorendonk, K. M., and Rabouille, C. (2005) *Mol. Biol. Cell* **16,** 4061–4072
15. Sengupta, D., Truschel, S., Bachert, C., and Linstedt, A. D. (2009) *J. Cell Biol.* **186,** 41–55
16. Kuo, A., Zhong, C., Lane, W. S., and Derynck, R. (2000) *EMBO J.* **19,** 6427–6439
17. Barr, F. A., Preisinger, C., Kopajtich, R., and Körner, R. (2001) *J. Cell Biol.* **155,** 885–891
18. Paulhe, F., Imhof, B. A., and Wehrle-Haller, B. (2004) *J. Biol. Chem.* **279,** 55545–55555
19. Ureña, J. M., Merlos-Suárez, A., Baselga, J., and Arribas, J. (1999) *J. Cell Sci.* **112,** 773–784
20. Crambert, G., Li, C., Swee, L. K., and Geering, K. (2004) *J. Biol. Chem.* **279,** 30888–30895
21. Boyle, L. H., Gillingham, A. K., Munro, S., and Trowsdale, J. (2006) *J. Immunol.* **176,** 6464–6472
22. Fernández-Larrea, J., Merlos-Suárez, A., Ureña, J. M., Baselga, J., and Arribas, J. (1999) *Mol. Cell* **3,** 423–433
23. Iodice, L., Sarnataro, S., and Bonatti, S. (2001) *J. Biol. Chem.* **276,** 28920–28926
24. Nufer, O., Guldbrandsen, S., Degen, M., Kappeler, F., Paccaud, J. P., Tani, K., and Hauri, H. P. (2002) *J. Cell Sci.* **115,** 619–628
25. Yao, R., Maeda, T., Takada, S., and Noda, T. (2001) *Biochem. Biophys. Res. Commun.* **286,** 771–778
26. Robitaille, J., MacDonald, M. L., Kaykas, A., Sheldahl, L. C., Zeisler, J., Dubé, M. P., Zhang, L. H., Singaraja, R. R., Guernsey, D. L., Zheng, B., Siebert, L. F., Hoskin-Mott, A., Trese, M. T., Pimstone, S. N., Shastry, B. S., Moon, R. T., Hayden, M. R., Goldberg, Y. P., and Samuels, M. E. (2002) *Nat. Genet.* **32,** 326–330
27. Xu, Q., Wang, Y., Dabdoub, A., Smallwood, P. M., Williams, J., Woods, C., Kelley, M. W., Jiang, L., Tasman, W., Zhang, K., and Nathans, J. (2004) *Cell* **116,** 883–895
28. de Iongh, R. U., Abud, H. E., and Hime, G. R. (2006) *Front. Biosci.* **11,** 2442–2464
29. Martire, G., Mottola, G., Pascale, M. C., Malagolini, N., Turrini, I., Serafini-Cessi, F., Jackson, M. R., and Bonatti, S. (1996) *J. Biol. Chem.* **271,** 3541–3547
30. Spatuzza, C., Renna, M., Faraonio, R., Cardinali, G., Martire, G., Bonatti, S., and Remondelli, P. (2004) *J. Biol. Chem.* **279,** 42535–42544
31. Marra, P., Maffucci, T., Daniele, T., Tullio, G. D., Ikehara, Y., Chan, E. K., Luini, A., Beznoussenko, G., Mironov, A., and De Matteis, M. A. (2001) *Nat. Cell Biol.* **3,** 1101–1113
32. Vasile, E., Perez, T., Nakamura, N., and Krieger, M. (2003) *Traffic* **4,** 254–272
33. Bonatti, S., Migliaccio, G., and Simons, K. (1989) *J. Biol. Chem.* **264,** 12590–12595
34. Mottola, G., Jourdan, N., Castaldo, G., Malagolini, N., Lahm, A., Serafini-Cessi, F., Migliaccio, G., and Bonatti, S. (2000) *J. Biol. Chem.* **275,** 24070–24079
35. Liou, W., Geuze, H. J., and Slot, J. W. (1996) *Histochem. Cell Biol.* **106,** 41–58
36. Slot, J. W., and Geuze, H. J. (1985) *Eur. J. Cell Biol.* **38,** 87–93
37. Pascale, M. C., Malagolini, N., Serafini-Cessi, F., Migliaccio, G., Leone, A., and Bonatti, S. (1992) *J. Biol. Chem.* **267,** 9940–9947
38. Gallione, C. J., and Rose, J. K. (1985) *J. Virol.* **54,** 374–382
39. Kuehn, M. J., and Schekman, R. (1997) *Curr. Opin. Cell Biol.* **9,** 477–483
40. Nishimura, N., and Balch, W. E. (1997) *Science* **277,** 556–558
41. Saito, K., Chen, M., Bard, F., Chen, S., Zhou, H., Woodley, D., Polischuk, R., Schekman, R., and Malhotra, V. (2009) *Cell* **136,** 891–902
42. Lotti, L. V., Torrisi, M. R., Erra, M. C., and Bonatti, S. (1996) *Exp. Cell Res.* **227,** 323–331
43. Mezzacasa, A., and Helenius, A. (2002) *Traffic* **3,** 833–849
44. Ronchi, P., Colombo, S., Francolini, M., and Borgese, N. (2008) *J. Cell Biol.* **181,** 105–118
45. Sönnichsen, B., Lowe, M., Levine, T., Jämsä, E., Dirac-Svejstrup, B., and Warren, G. (1998) *J. Cell Biol.* **140,** 1013–1021
46. Hobbie, L., Fisher, A. S., Lee, S., Flint, A., and Krieger, M. (1994) *J. Biol. Chem.* **269,** 20958–20970
47. Slusarski, D. C., Corces, V. G., and Moon, R. T. (1997) *Nature* **390,** 410–413
48. Kaykas, A., Yang-Snyder, J., Héroux, M., Shah, K. V., Bouvier, M., and Moon, R. T. (2004) *Nat. Cell Biol.* **6,** 52–58
49. Standley, S., Roche, K. W., McCallum, J., Sans, N., and Wenthold, R. J. (2000) *Neuron* **28,** 887–898
50. Wenthold, R. J., Prybylowski, K., Standley, S., Sans, N., and Petralia, R. S. (2003) *Annu. Rev. Pharmacol. Toxicol.* **43,** 335–358
51. Ward, T. H., Polishchuk, R. S., Caplan, S., Hirschberg, K., and Lippincott-Schwartz, J. (2001) *J. Cell Biol.* **155,** 557–570
52. Parnes, J. R. (1989) *Adv. Immunol.* **44,** 265–311
53. Devine, L., Kieffer, L. J., Aitken, V., and Kavathas, P. B. (2000) *J. Immunol.* **164,** 833–838
54. Dialynas, D. P., Loken, M. R., Glasebrook, A. L., and Fitch, F. W. (1981) *J. Exp. Med.* **153,** 595–604
55. DiSanto, J. P., Knowles, R. W., and Flomenberg, N. (1988) *EMBO J.* **7,** 3465–3470
56. Norment, A. M., and Littman, D. R. (1988) *EMBO J.* **7,** 3433–3439
57. Hennecke, S., and Cosson, P. (1993) *J. Biol. Chem.* **268,** 26607–26612
58. Schmidt-Ullrich, R., and Eichmann, K. (1990) *Int. Immunol.* **2,** 247–256